Electronic Supplementary Material (ESI) for Chemical Communications
This journal is © The Royal Society of Chemistry 2015

Facile Synthesis of $NiCoMnO_4$ Nanoparticles as Novel Electrode Materials for High-Performance Asymmetric Energy Storage Devices

Afshin Pendashteh,[a,*] Jesus Palma,[a] Marc Anderson,[a,b] and Rebeca Marcilla [a]

[a] *Electrochemical Processes Unit, IMDEA Energy Institute, Parque Tecnológico de Móstoles Avda. Ramón de la Sagra, 3, 28935 Móstoles, Madrid, Spain.*
[b] *Department of Civil and Environmental Engineering, University of Wisconsin, Madison, USA*
* *To whom correspondence should be sent, Email: afshin.pendashteh@imdea.org*

Electronic Supplementary Information (ESI†)

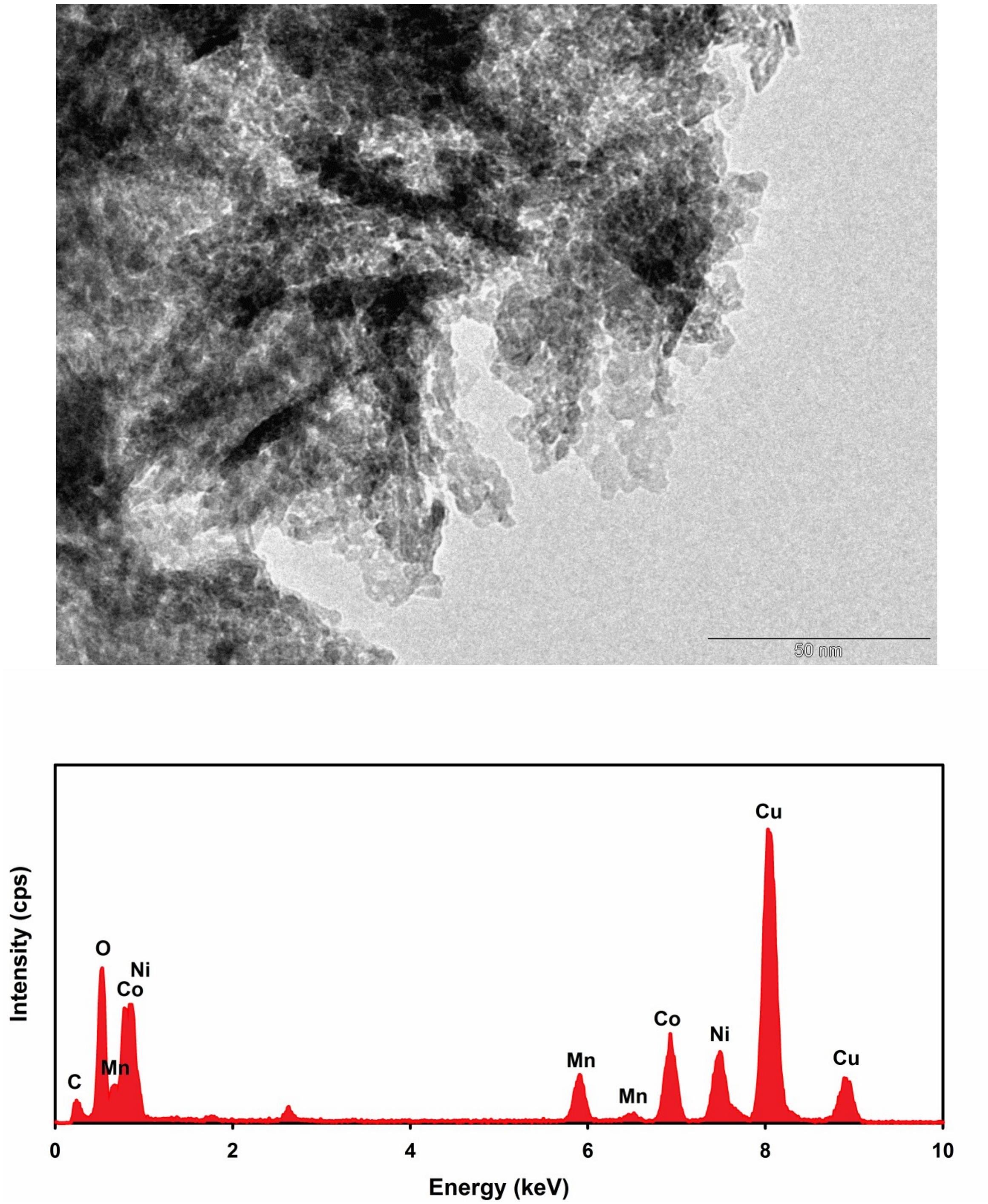

Figure S1. EDX spectrum of $NiCoMnO_4$ nanoparticles (NCMO NPs) along with the corresponding TEM image from which the spectrum was collected. Carbon and copper signals originated from the used grid (polymer coated copper grid) as the sample holder.

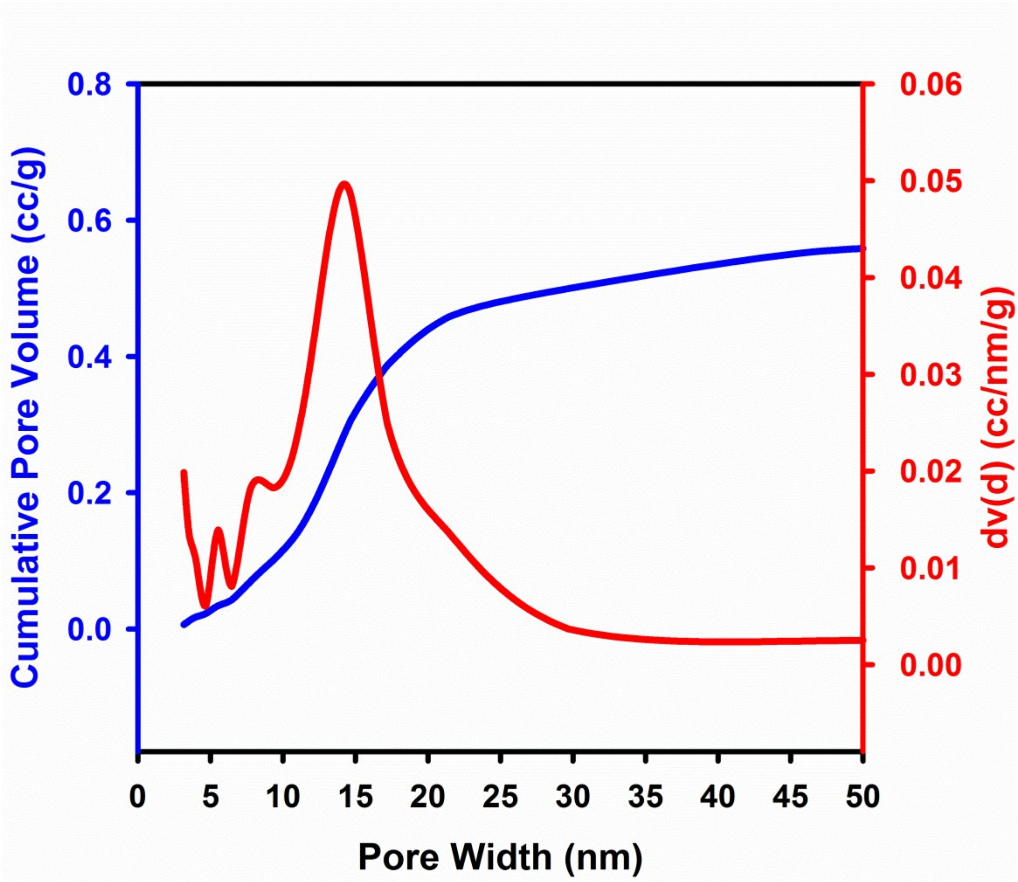

Figure S2. Pore size distribution of $NiCoMnO_4$ nanoparticles (NCMO NPs) calculated based on BJH theory.

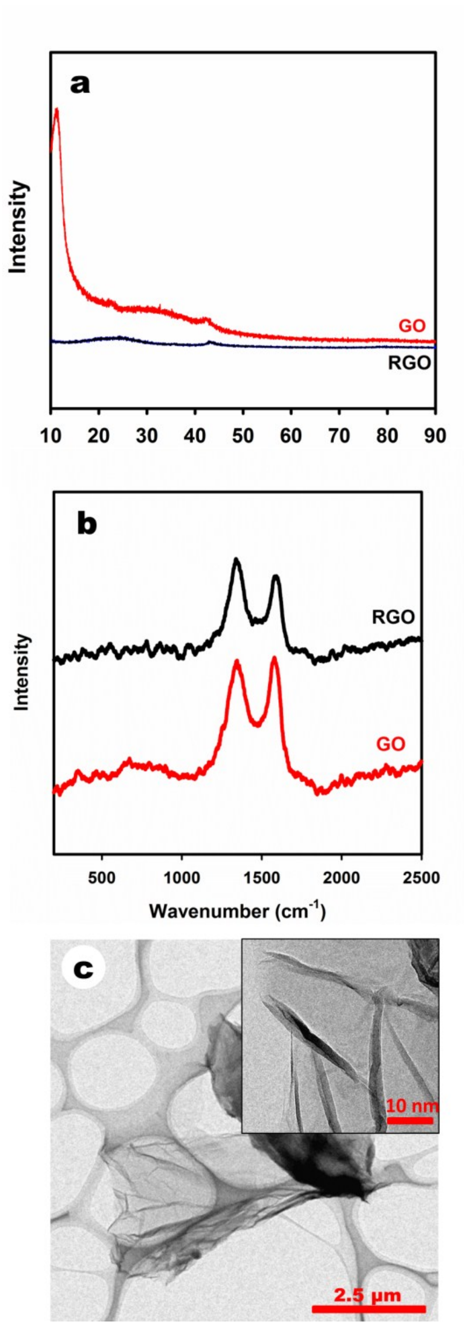

Figure S3. (a) XRD patterns, and (b) Raman spectra of GO and RGO samples. (c) TEM images of RGO NSs on a polymeric network grid as sample holder).

In XRD (S3a), sharp intense peak at around 11.4° confirms high degree of oxidation of graphite layers, reflected in increased interlayer spacing (e.g. 7.58 Å). This is while that in RGO only a broad low-intense peak arose at 24.72°, corresponding to basal reflection of (002) plane.

In Raman spectra (S3b), two characteristic peaks, referred to D (1335 cm^{-1}) and G (1595 cm^{-1}) bands are clearly seen. D-band originates from the structural defects on the carbon basal plane while the G-band is assigned to the first-order scattering of E_{2g} phonon from sp^2 carbon.

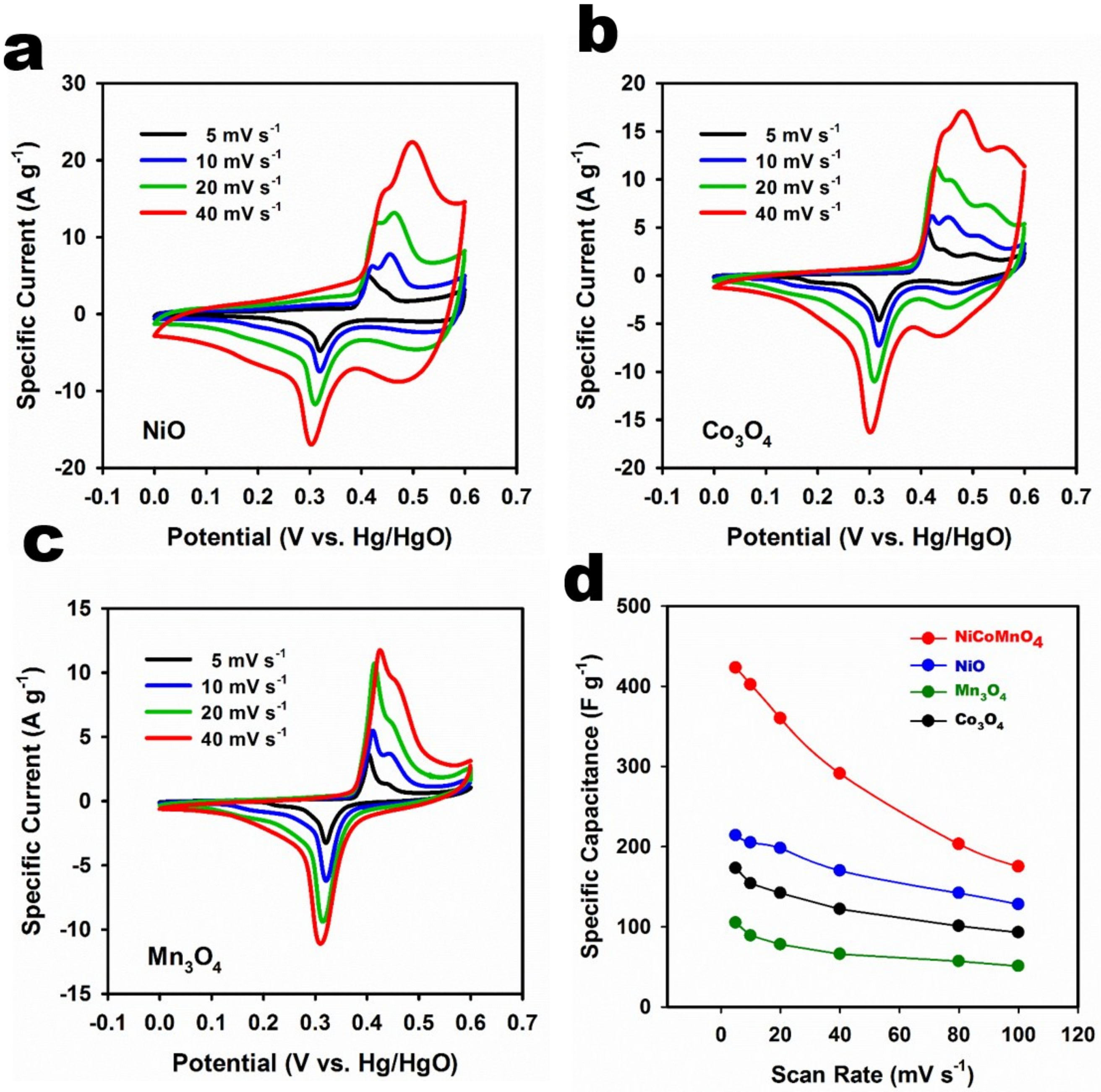

Figure S4. Cyclic voltammograms of (a) NiO, (b) Co_3O_4, (c) Mn_3O_4, and (d) their specific capacitances in comparison with $NiCoMnO_4$ sample at various scan rates.

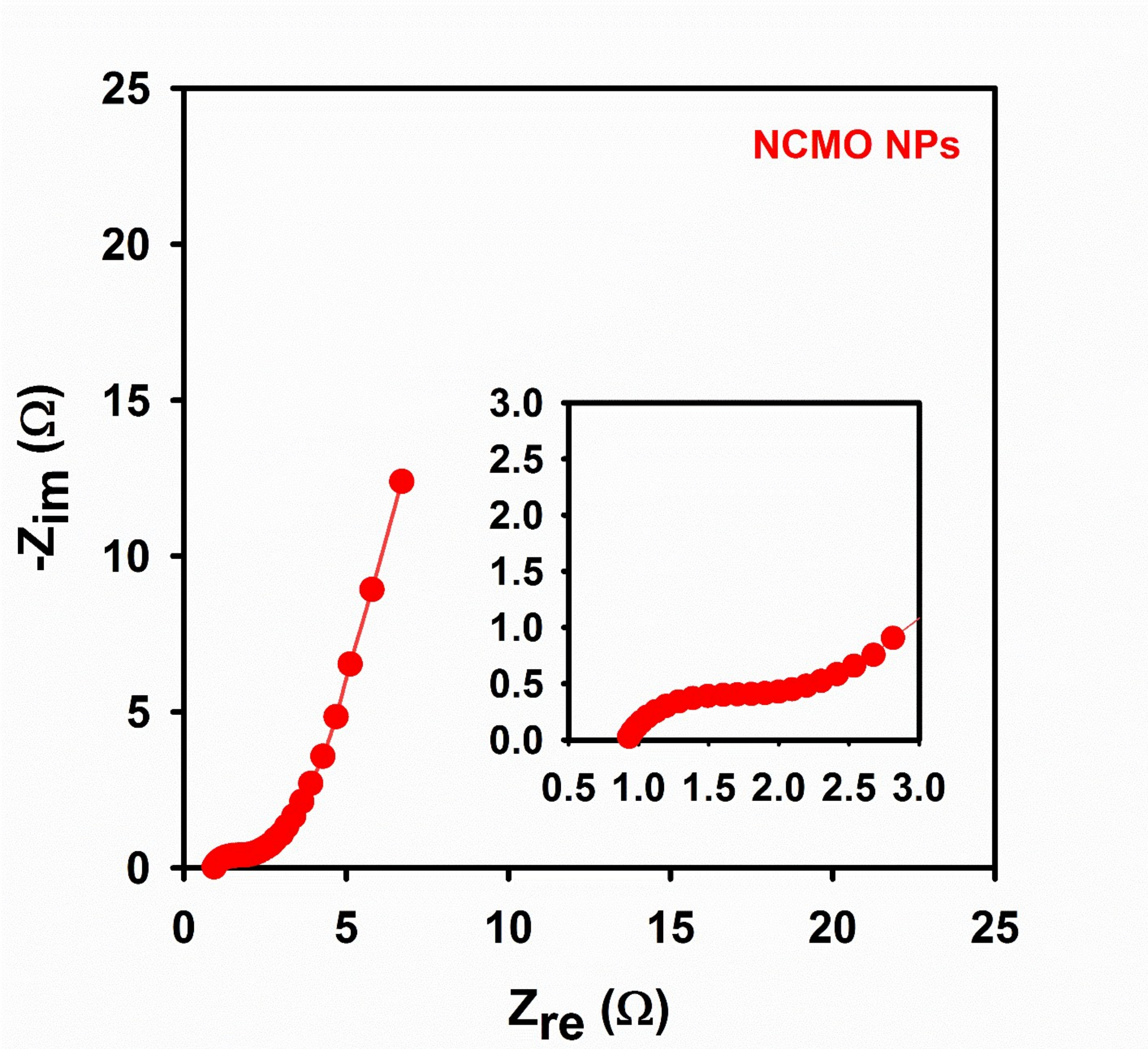

Figure S5. Nyquist plot of $NiCoMnO_4$ electrodes.

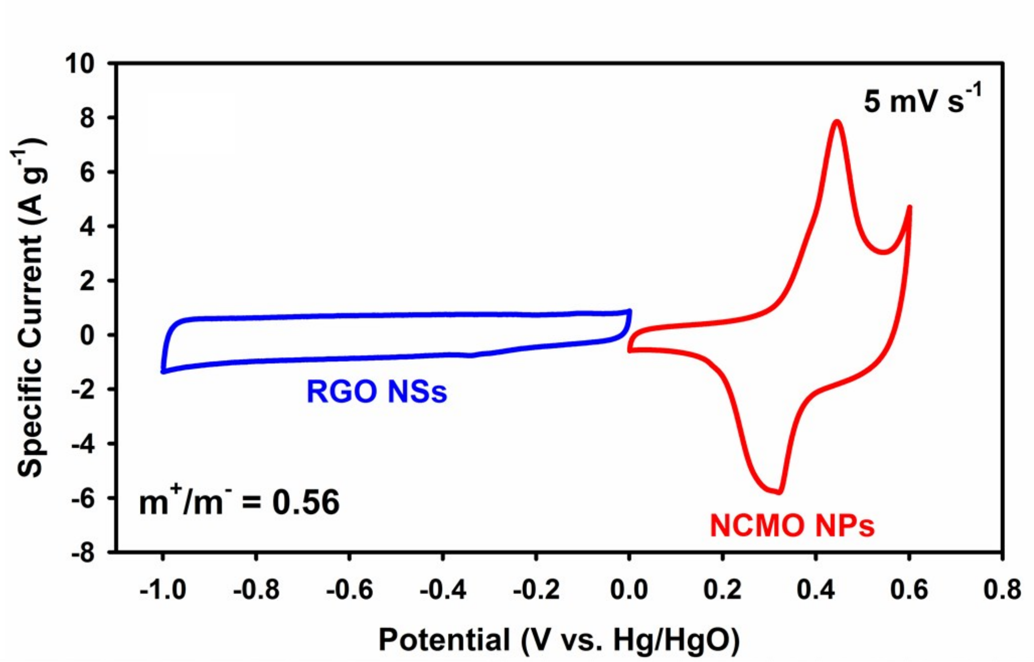

Figure S6. (a) Cyclic voltammetry of NCMO NPs and RGO NSs electrodes in a 3 electrode configuration at 5 mV.s^{-1}, showing the possibility of expanding working potential window by integrating electrodes.

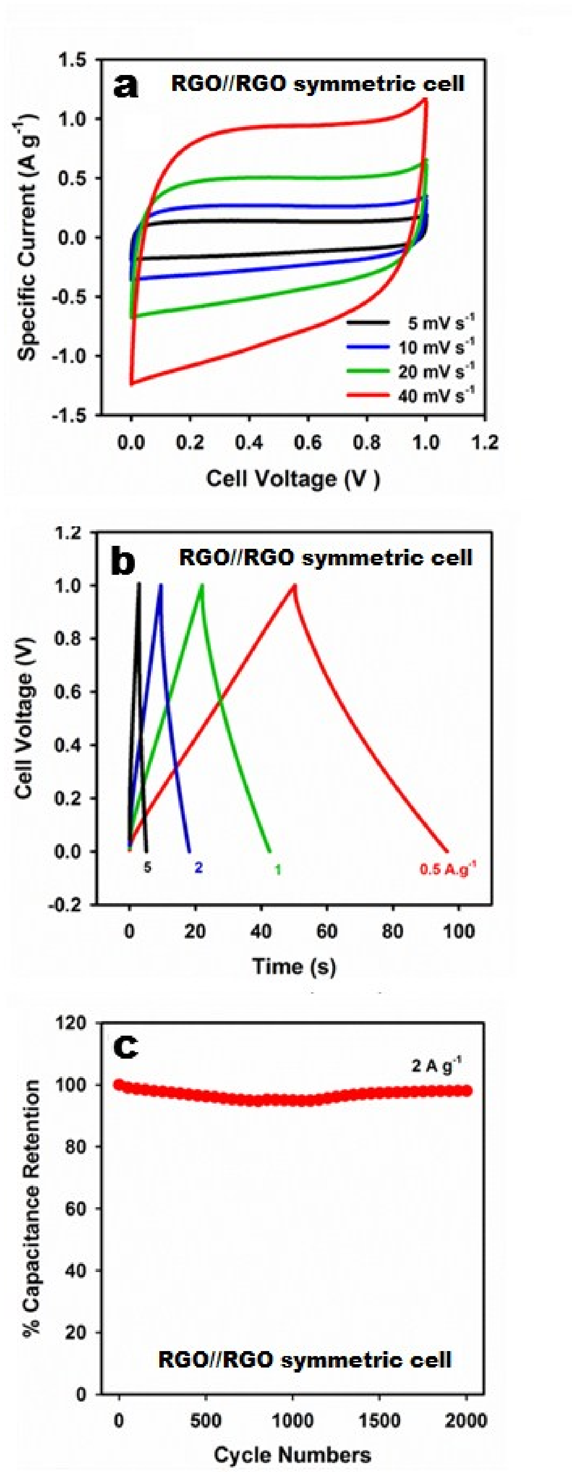

Figure S7. Electrochemical evaluation of symmetric RGO//RGO supercapacitors: (a) CVs at various scan rates; (b) GCD profiles of the symmetric device at various specific currents; and (c) cycling performance of the cell at 2 A.g^{-1} over 2000 cycles.

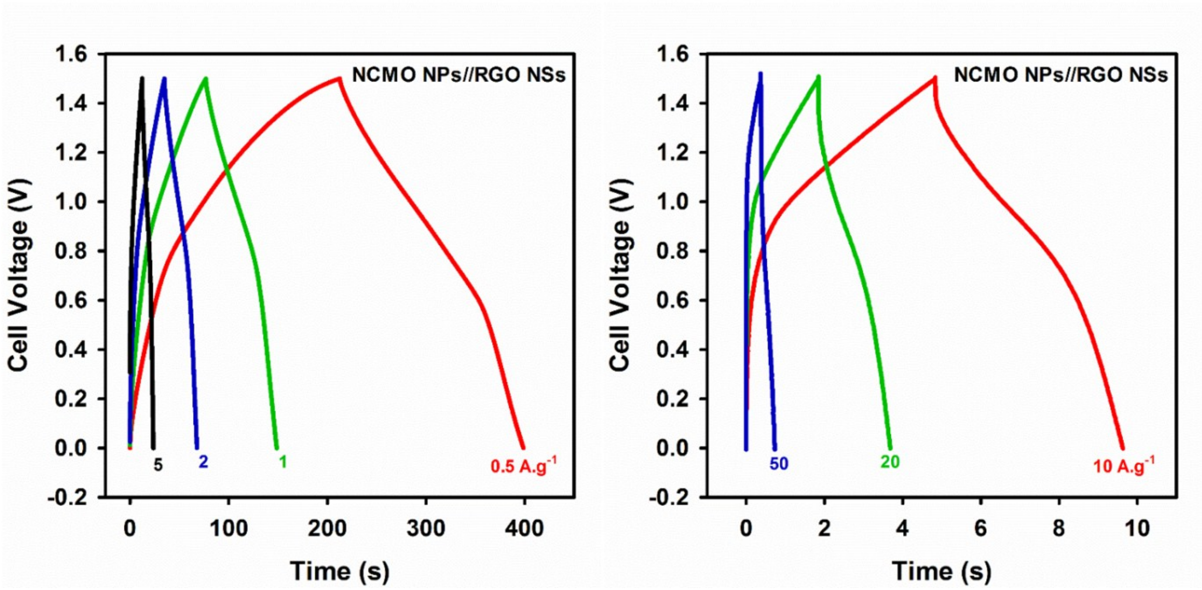

Figure S8. Charge-discharge profiles of the hybrid NCMO NPs//RGO NSs cells at various specific currents.